LETTERS

Clustered DNA motifs mark X chromosomes for repression by a dosage compensation complex

Patrick McDonel[1,2]*, Judith Jans[1,2]*, Brant K. Peterson[2] & Barbara J. Meyer[1,2]

Gene expression in metazoans is regulated not only at the level of individual genes but also in a coordinated manner across large chromosomal domains (for example centromeres, telomeres and imprinted gene clusters[1–3]) and along entire chromosomes (for example X-chromosome dosage compensation[4–6]). The primary DNA sequence usually specifies the regulation of individual genes, but the nature of *cis*-acting information that controls genes over large regions has been elusive: higher-order DNA structure, specific histone modifications, subnuclear compartmentalization and primary DNA sequence are possibilities. One paradigm of chromosome-wide gene regulation is *Caenorhabditis elegans* dosage compensation in which a large dosage compensation complex (DCC) is targeted to both X chromosomes of hermaphrodites to repress transcript levels by half[6]. This essential process equalizes X-linked gene expression between the sexes (XO males and XX hermaphrodites). Here we report the discovery and dissection of *cis*-acting sites that mark nematode X chromosomes as targets for gene repression by the DCC. These *rex* (recruitment element on X) sites are widely dispersed along X and reside in promoters, exons and intergenic regions. *rex* sites share at least two distinct motifs that act in combination to recruit the DCC. Mutating these motifs severely reduces or abolishes DCC binding *in vivo*, demonstrating the importance of primary DNA sequence in chromosome-wide regulation. Unexpectedly, the motifs are not enriched on X, but altering motif numbers within *rex* sites demonstrates that motif co-occurrence in unusually high densities is essential for optimal DCC recruitment. Thus, X-specific repression is established through sequences not specific to X. The distribution of common motifs provides the foundation for repression along an entire chromosome.

The *C. elegans* DCC resembles condensin, a conserved protein complex required for mitotic and meiotic chromosome compaction, resolution and segregation[7–9]. Participation of condensin and condensin-like proteins in gene regulation extends beyond dosage compensation, to transcriptional silencing in yeast[10] and position-effect variegation in flies[11,12], suggesting a general role for these proteins in establishing and maintaining a repressed state.

Our goals were to identify X chromosome sites responsible for DCC recruitment and to define molecular features within these *rex* sites critical for target recognition and DCC binding. Previous work surveyed large regions of X (1–10 million base pairs (Mbp)) for their abilities to recruit the DCC when detached from X[13]. Some detached regions recruited the DCC but others did not, yet the DCC localized to all corresponding regions of the intact X (Fig. 1a), suggesting that recruitment sites are widely distributed along X to bind the DCC and nucleate DCC spreading to X regions lacking recruitment sites[13].

To identify specific *rex* sites, we generated transgenic nematode lines carrying extrachromosomal arrays containing multiple copies of individual X-chromosome cosmids sampled from large DCC-recruiting regions (Fig. 1a). DCC recruitment to arrays was examined in intestinal cell nuclei by using fluorescence *in situ* hybridization to mark array position and antibodies against dosage compensation proteins to mark DCC location[13] (Supplementary Fig. 1a). The first four positive cosmids identified were dissected further by assaying successively smaller sub-cosmid fragments to define the minimal DNA fragments, and ultimately the shared *cis*-acting motifs, responsible for optimal DCC binding.

Full recruitment ability was ascribed to 241 base pairs (bp) for *rex-1*, 147 bp for *rex-2*, 115 bp for *rex-3*, and 411 bp for *rex-4* (Table 1, Fig. 1a, b, and Supplementary Methods). Arrays containing only 33 bp of *rex-1* recruited the DCC robustly in all nuclei, although arrays of larger *rex-1* fragments (60–241 bp) had stronger DCC recruitment activity (Fig. 2). No bias was found in the location of *rex* sites relative to coding sequences: both *rex-1* and *rex-2* reside in intergenic regions, *rex-3* in an exon, and *rex-4* in a promoter. Furthermore, *rex* sites seem widely spaced: *rex-3* is flanked by at least 300 kb of non-recruiting DNA and *rex-4* by a minimum of 100 kb.

DCC binding to *rex* arrays mimics DCC binding to intact X chromosomes. First, binding to *rex-1* requires SDC-2, the hermaphrodite-specific dosage compensation protein that triggers the binding of all DCC proteins to X and binds X without other DCC components, notably SDC-3, its partner in recruitment[6,14]. In *sdc-2* mutants, neither DCC subunit SDC-3 nor DPY-27 was detected on arrays (Supplementary Fig. 1a, b). Furthermore, in *sdc-3* mutants, SDC-2—but not DPY-27—bound *rex-1* arrays (Supplementary Fig. 1c). Second, *rex-1* sites integrated at low copy number into autosomes recruit the DCC (Supplementary Fig. 1d). No significant DCC spreading was detected in flanking autosomal chromatin, perhaps indicating the absence of DNA sequences required for spreading or, alternatively, the presence of nearby inhibitory DNA sequences, proteins or chromatin modifications.

Sequence analysis of *rex-1* to *rex-4* with the use of MEME[15] revealed multiple occurrences of two short degenerate DNA motifs clustered within each *rex* site, namely motif A (C/GCAGGGG) and motif B (T/GGTAATTG) (Fig. 1b, c, Methods, Supplementary Table 1 and Supplementary Methods). A and B motifs occur in the four *rex* sites (totalling 914 bp) at frequencies more than 20-fold greater ($P < 10^{-10}$) than empirically determined whole-genome frequencies. In contrast, the motifs are not significantly overrepresented in 16 X-linked cosmids that failed to recruit the DCC (totalling 535 kb) or in a set of smaller non-recruiting X fragments (totalling 23 kb) similar in size to *rex* sites. Despite occurrences at unusually high frequencies in *rex* sites, A motifs are not found more frequently on X than on autosomes, and B motifs are only slightly (1.25-fold) enriched on X.

[1]Howard Hughes Medical Institute and [2]Department of Molecular and Cell Biology, University of California – Berkeley, 16 Barker Hall Berkeley, California 94720-3204, USA.
*These authors contributed equally to this work.

Computational comparisons showed the overall density of 600-bp windows containing both A and B motifs is a strong discriminator ($P < 0.003$) between *rex* cosmids (higher density) and non-recruiting X cosmids or autosomes or even the entire X chromosome (all lower density). The discrimination between these data sets is even more apparent ($P < 0.001$) when the windows are assessed by the sum of scores for the two motifs (Supplementary Methods). Among many models tested, one that best discriminates between recruiting and non-recruiting cosmids in our training set (4 *rex* cosmids and 16 non-*rex* cosmids) predicts that a cosmid with at least one A and one B motif, each with a raw motif score of 8.0 or more and clustered within a 600-bp window, should recruit the DCC.

Applying these parameters to 30-kb segments tiling the entire X, we observed a non-uniform distribution of predicted positive segments among known[13] strongly recruiting, weakly recruiting and non-recruiting regions of X (Fig. 1d, and Supplementary Fig. 2). Recruiting regions are significantly enriched for predicted positive windows relative to non-recruiting regions ($P < 0.004$; Supplementary Table 2). Thus, the distribution of high-scoring motif A and B clusters on X corresponds well to previous[13] DCC recruitment studies.

The utility of this model was assessed by predicting and assaying recruitment abilities of individual cosmids covering a 2-Mbp region of X, including region D and part of C (Fig. 1a) but excluding the training set. Four of nine positive cosmid predictions proved correct, demonstrating a true positive prediction frequency of 0.44. In addition, 27 of 34 predictions correctly identified non-recruiting cosmids. The probability of selecting a true positive cosmid in this region by chance is 0.22, because 13 of 58 total cosmids (including the training set) recruited. Thus, even this simple model using high-scoring A and B motif clusters improves positive cosmid prediction.

The functional significance of A and B motifs in DCC recruitment was established through mutational analysis of *rex* sites (Table 1, Fig. 2, Supplementary Table 1 and Supplementary Figs 3 and 4). (See Table 1 legend for nomenclature.) Recruitment *in vivo* was judged by two parameters: percentage of array-bearing nuclei with a DCC-recruiting array, and strength of DCC recruitment to arrays compared with recruitment to X chromosomes. Five recruitment strengths could be distinguished qualitatively (Fig. 2). Category 0 arrays never recruited the DCC. Category 1 arrays had infrequent, patchy DCC co-localization; X staining was bright. Category 2 arrays had consistently robust DCC staining but not significantly brighter than X staining. Category 3 arrays recruited so strongly they competed with X for the limited pool of DCC and appeared brightly stained relative to the faint (category 3^-) or undetectable (category 3) X chromosomes. Wild-type *rex-1*•241, *rex-3*•115 and *rex-4*•411 arrays are of category 3 (100% recruiting nuclei); wild-type *rex-1*•33 and *rex-2*•147 arrays are of category 2 (100% recruiting nuclei).

Motif A is critical for DCC recruitment (Table 1). Mutating six nucleotides of the single A motif in either the 33-bp *rex-1* fragment (*rex-1*•33mA_1), the 147-bp *rex-2* fragment (*rex-2*•147mA_1) or the 115-bp *rex-3* fragment (*rex-3*•115mA_1) abolished DCC recruitment (category 0; Fig. 2b, and Supplementary Figs 3 and 4b, c). In fact, DCC recruitment to *rex-1* was severely impaired by just a 2-bp substitution in motif A (category 1, 17% recruiting nuclei; Supplementary Fig. 4b). *rex-4* has two A motifs, and recruitment was disrupted only when both motifs (*rex-4*•411mA_1A_2) were mutated (category 2, 20% recruiting nuclei; Supplementary Fig. 4c).

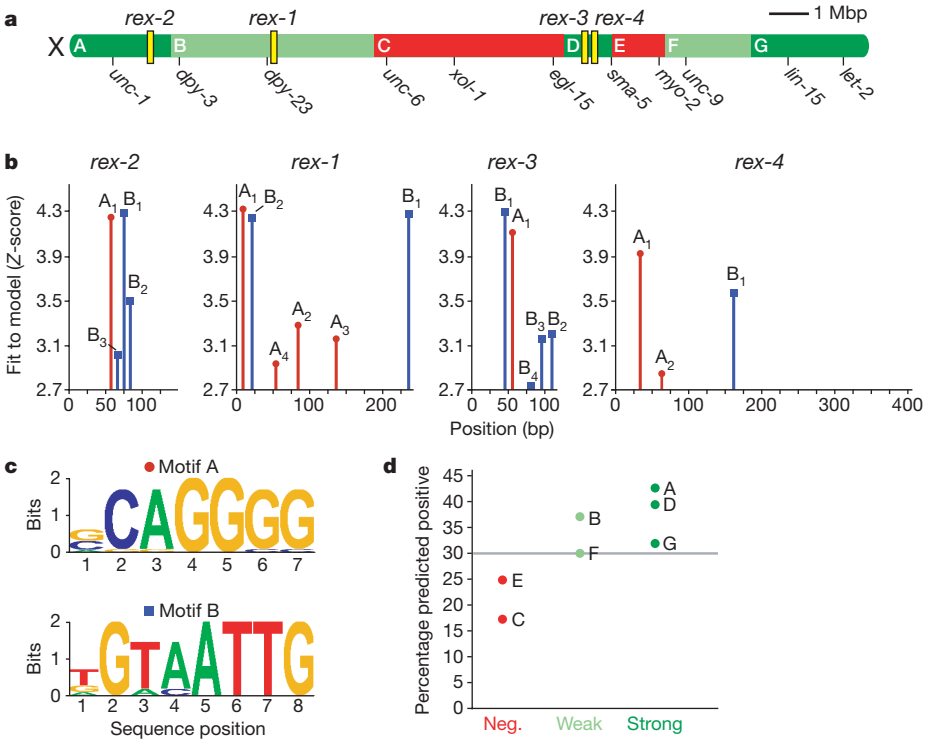

Figure 1 | DCC recruitment elements on X (*rex* sites) contain clusters of *cis*-acting regulatory motifs. **a**, DCC recruitment map of the *C. elegans* X chromosome. The positions of dissected *rex* sites (yellow) are indicated relative to previously determined X regions[13] that strongly recruit (dark green), weakly recruit (light green) or fail to recruit (red) the DCC when detached from X. **b**, Positions of *cis*-regulatory motifs A (red circles) and B (blue squares) and their corresponding *Z*-scores in each full-strength *rex* site (241 bp for *rex-1*, 147 bp for *rex-2*, 115 bp for *rex-3*, and 411 bp for *rex-4*). *Z*-scores for every nucleotide position were calculated as (raw score minus mean score)/(standard deviation of all scores). Raw scores were generated by comparing every window of seven or eight nucleotides to position weight matrices (PWMs) for motif A and motif B. Within a *rex* site, individual A and B motifs were named according to their relative scores against the PWMs, with A_1 and B_1 being the best scoring instances per site (see Supplementary Table 1). **c**, Models describing *cis*-acting regulatory motifs A and B based on PWMs. **d**, Plot showing correspondence between a predictive model for DCC recruitment (see the text) and previous[13] X-chromosome-wide recruitment data. The percentage of predicted positive 30-kb segments is significantly greater in strongly (A, D and G; dark green) and weakly (B and F; light green) recruiting X regions than in non-recruiting regions (C and E; red) ($P < 0.004$; see Supplementary Table 2). The percentage of positive windows predicted for the entire X is 30% (grey line).

Motif B is also important for DCC recruitment (Table 1). Altering the single B motif in *rex-1* (*rex-1*•33mB_2) nearly eliminated DCC binding (category 1, 9% recruiting nuclei), and altering the single B motif in *rex-4* (*rex-4*•411mB_1) severely reduced binding (category 2, 32% recruiting nuclei; Supplementary Fig. 4d). In contrast, mutating six nucleotides not overlapping either motif A or B in *rex-1*•33 (*rex-1*•33m control) had little effect (category 2, 96% recruiting nuclei), confirming specificity in disrupting DCC binding (Supplementary Fig. 4b).

Strength of DCC recruitment to *rex-1* fragments is correlated with motif number. Arrays carrying the minimal fragment *rex-1*•33 (1A,1B motifs) exhibited category 2 recruitment with obvious X staining, indicating the inability to outcompete X for DCC binding, whereas arrays of *rex-1*•241 (4A,2B motifs) exhibited category 3 recruitment with undetectable X staining, indicating that X was deprived of DCC binding (Table 1 and Fig. 2a, f). This distinction was evident in both polyploid cells of adult intestines (Fig. 2) and diploid cells of young embryos (Supplementary Fig. 5), when dosage compensation is first established. Thus, *rex-1*•241 arrays should disrupt dosage compensation to a greater extent than *rex-1*•33 arrays, a prediction confirmed by genetic assays below.

Mutations in the sex-determination gene *xol-1* cause complete male lethality from inappropriate DCC binding to the single male X and the consequent reduction of gene expression[7,16]. *xol-1* mutant males can be rescued by disrupting DCC components[16] or by titrating the DCC from X with a new target such as a *rex* array[13]. The extent of male rescue should correlate with the target's ability to compete with X for DCC binding. We found that *rex-1*•33 arrays (category 2) failed to rescue *xol-1* male lethality, as did *rex-1*•60 arrays (category 3^-), but *rex-1*•148 arrays (category 3) rescued 55% of *xol-1* males, and *rex-1*•241 arrays (category 3) rescued 98% (Supplementary Methods).

Whereas reduction in DCC binding to the male X increases male viability, reduction in binding to hermaphrodite X chromosomes

Table 1 | Motifs A and B act in combination and are crucial for DCC recruitment to *rex* sites

Construct*	No. of wild-type motifs	Recruitment strength†	Recruitment (%)‡	No. of nuclei (no. of lines)§
rex-1				
rex-1 cosmid R160	213A,397B	2	94	35 (2)
rex-1•33wt	1A,1B	2	100	>50 (2)
rex-1•33mA_1	0A,1B	0	0	55 (3)
rex-1•33mA_1 (GttGGGG)	0A,1B	1	17	57 (2)
rex-1•33mA_1 (GCAttGG)	0A,1B	1	41	58 (3)
rex-1•33mA_1 (GCAGGtt)	0A,1B	1	22	52 (3)
rex-1•33mB_2 (GTACCAAA)	1A,0B	1‖	9	39 (2)
rex-1•33mControl¶	1A,1B	2	96	30 (2)
rex-1•60wt	2A,1B	3^-	100	>50 (2)
rex-1•60mA_1	1A,1B	2	100	69 (3)
rex-1•60mA_1A_4	0A,1B	1	33	52 (2)
rex-1•89wt	3A,1B	3	100	47 (2)
rex-1•89mA_1	2A,1B	3^-	100	53 (2)
rex-1•148wt	4A,1B	3	100	>50 (2)
rex-1•148mA_1	3A,1B	3	100	44 (2)
rex-1•148mA_1A_3	2A,1B	3^-	100	37 (2)
rex-1•148m$A_1A_3A_4$	1A,1B	2	100	60 (3)
rex-1•148m$A_1A_2A_3A_4$	0A,1B	1	36	61 (3)
rex-1•148mB_2 (GTACCAAA)	4A,0B	2	100	28 (2)
rex-1•241wt	4A,2B	3	100	>50 (2)
rex-1•241mA_1	3A,2B	3	100	43 (2)
rex-1•241mB_2 (GTACCAAA)	4A,1B	2	100	68 (2)
rex-2				
rex-2 cosmid B0294	154A,433B	2	100	>50 (2)
rex-2•147wt	1A,3B	2	100	63 (2)
rex-2•147mA_1	0A,3B	0	0	41 (2)
rex-3				
rex-3 cosmid F42E11	89A,331B	2	100	40 (2)
rex-3•115wt	1A,4B	3	100	>50 (2)
rex-3•115mA_1	0A,4B	0	0	>50 (2)
rex-3•115mB_1	1A,3B	3	100	>50 (3)
rex-3•115mB_1B_2	1A,2B	3^-	95	38 (3)
rex-3•115m$B_1B_2B_3$	1A,1B	2	70	90 (3)
rex-3•115m$B_1B_2B_3B_4$	1A,0B	2	15	74 (3)
rex-4				
rex-4 cosmid F29G6	99A,349B	2	94	35 (2)
rex-4•411wt	2A,1B	3^-	100	35 (2)
rex-4•411mA_1	1A,1B	3^-	100	>100 (2)
rex-4•411mA_1A_2	0A,1B	2	20	24 (2)
rex-4•411mB_1	2A,0B	2	32	60 (3)

The table shows the specific effects on DCC recruitment of multiple A and B motifs within each *rex* site and the effects of subsequent mutation of these motifs. *rex* arrays were scored for DCC binding by using two parameters, namely recruitment strength to an array and percentage of array-bearing nuclei with a recruiting array (described in the text). Increasing the number of motifs by a stepwise extension of *rex-1* from 33 bp (*rex-1*•33wt) through 60, 89 and 148 bp to 241 bp (*rex-1*•241wt) improved both recruitment strength and percentage recruitment. The enhanced recruitment was abolished on subsequent mutation of the added motifs, revealing the central role of these motifs in DCC recruitment. These results confirm the functional importance of A and B motifs in DCC recruitment and highlight the role of motif density. The *rex-1* fragments with identical numbers of A and B motifs exhibited similar recruitment strengths. Arrays from *rex-1* fragments with one A motif and one B motif (*rex-1*•33, *rex-1*•60mA_1 and *rex-1*•148m$A_1A_3A_4$) were in category 2; those with two A motifs and one B motif (*rex-1*•60, *rex-1*•89mA_1 and *rex-1*•148mA_1A_3) were in category 3^- with faint X staining; and those with three A motifs and one B motif (*rex-1*•148mA_1 and *rex-1*•89) were in category 3 with undetectable X staining.

* Nomenclature for *rex* sites is exemplified by *rex-1*•148m$A_1A_3A_4$, which indicates that motifs A_1, A_3 and A_4 have been mutated in the 148-bp *rex-1* fragment. 'm' precedes the complete list of mutant motifs. For mutational analysis, positions 2–7 of motif A (G/CCAGGG) were changed to TTTTTT, and positions 2–8 of motif B (T/GTAATTG) were changed to TTTTTTT, except where specifically noted in parentheses. Sequences of all wild-type and mutant motifs are given in Supplementary Table 1.

† Strength of DCC recruitment to an array compared with recruitment to X chromosomes. Category 0, never recruit DCC to array; category 1, infrequent and patchy DCC localization to array; category 2, robust DCC recruitment to all arrays with staining not brighter than X staining; category 3^-, robust DCC recruitment to all arrays with faint X staining; category 3, robust DCC recruitment to all arrays with undetectable X staining.

‡ Percentage of array-bearing nuclei with a DCC recruiting array.

§ Total number of array-bearing nuclei scored. The number of independent transgenic lines is given in parenthesis.

‖ No recruitment in one line and very weak recruitment in the other.

¶ In this control, GCTGCG was changed to TTATTT.

should lower hermaphrodite viability. Indeed, 31% of hermaphrodites carrying *rex-1*•241 arrays died from defective dosage compensation, and escapers exhibited a partial disruption of dosage compensation. In contrast, only 10% of *rex-1*•33-bearing hermaphrodites died, and escapers seemed normal. These combined genetic results corroborate our cytological evidence that *rex-1* fragments with more motifs elicit stronger DCC recruitment.

To determine whether the enhanced recruitment strength of *rex-1*•241 compared with that of *rex-1*•33 was due to additional A motifs, we assayed a series of *rex-1* fragments of increasing size, such that each progressively larger fragment included one additional A motif. Contributions of specific A motifs were then verified by mutational analysis (Table 1, Fig. 2, Supplementary Table 1 and Supplementary Fig. 4a, b). Extending *rex-1* from 33 bp to 60 bp (*rex-1*•60, with 2A,1B motifs) added one A motif (A_4) and markedly increased DCC recruitment strength from category 2 to 3^-. Mutating an A motif (A_1) in *rex-1*•60 to generate *rex-1*•60mA_1 (1A,1B motifs) returned recruitment strength to category 2, the strength of *rex-1*•33. Mutating the remaining A motif (A_4) to generate *rex-1*•60mA_1A_4 (0A,1B motifs) reduced recruitment strength further, to category 1, establishing that A_4 was responsible for the enhanced DCC binding to *rex-1*•60 compared with *rex-1*•33.

Increasing the number of A motifs in *rex-1* to three (*rex-1*•89, with 3A,1B motifs) or four (*rex-1*•148, with 4A,1B motifs) strengthened recruitment to category 3, making it indistinguishable from that of *rex-1*•241 (4A,2B motifs). As expected, mutating one motif (A_1) in *rex-1*•89 to generate *rex-1*•89mA_1 (2A,1B motifs) and mutating two motifs (A_1 and A_3) in *rex-1*•148 to yield *rex-1*•148mA_1A_3 (2A,1B motifs) reduced recruitment strength to that of *rex-1*•60 (2A, 1B motifs; category 3^-). Mutating a third motif (A_4) in *rex-1*•148 (*rex-1*•148m$A_1A_3A_4$, with 1A,1B motifs) reduced recruitment strength to category 2 (100% recruiting nuclei), and mutating the fourth motif (A_2) to generate *rex-1*•148m$A_1A_2A_3A_4$ (0A,1B motifs) reduced recruitment strength to category 1 (36% recruiting nuclei).

In summary, *rex-1* fragments with identical numbers of A and B motifs had similar recruitment strengths, and DCC recruitment to *rex-1* was markedly improved by the increased occurrence of A motifs. The degree of improvement in DCC binding indicates that A motifs might act cooperatively.

B motifs seem additive in function. Disrupting the highest-scoring B motif in *rex-3* (*rex-3*•115mB_1, with 1A,3B motifs) had no discernible effect on DCC binding, disrupting two B motifs (*rex-3*•115mB_1B_2, with 1A,2B motifs) had a minor effect, disrupting three B motifs (*rex-3*•115m$B_1B_2B_3$, with 1A,1B motifs) caused substantial reduction, and disrupting all four B motifs eliminated most DCC binding (Table 1 and Supplementary Fig. 4d). These results, together with the enhanced recruitment to *rex-1* conferred by multiple A motifs, show that although a single A and B motif pair is sufficient to attract the DCC in our array assay (as in *rex-1*•33), optimal recruitment is attained only when multiple motifs are present (as in *rex-1*•241 and *rex-3*•115). On the native X chromosome, a recruitment site with a higher density of motifs, even those with lower scores, is more likely to attract the DCC than a site with a lower motif density.

Although A and B motifs act in combination, A motifs can compensate, although not completely, for the loss of motif B (Table 1 and

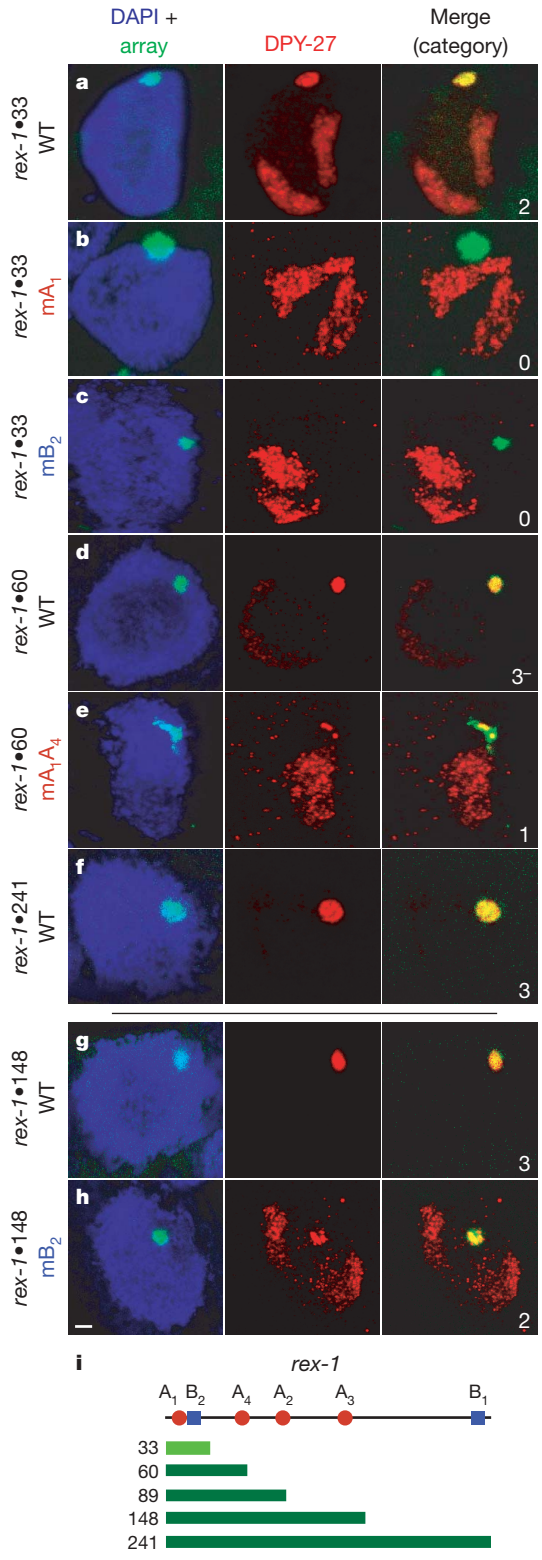

Figure 2 | Mutational analysis of *rex-1* establishes motifs A and B as *cis*-acting regulatory elements critical for DCC recruitment. Confocal images of intestinal cell nuclei (4,6-diamidino-2-phenylindole (DAPI) stain, blue) carrying wild-type (WT; **a**, **d**, **f**, **g**) or mutant (**b**, **c**, **e**, **h**) *rex* arrays (fluorescence *in situ* hybridization, green) co-stained with DPY-27 antibodies (red). DPY-27 binding to X requires all other known DCC components. The recruitment strength category (see the text for description) of each array is indicated by a number (0–3) at the right. **a**, Arrays containing a cloned 33-bp *rex-1* fragment (1A,1B motifs) recruit the DCC robustly. **b**, **c**, Mutating either motif A (**b**) or motif B (**c**) in *rex-1*•33 abolishes DCC recruitment. (See also Supplementary Fig. 1.) **d**, Extending *rex-1* to 60 bp adds a second motif A and markedly increases recruitment strength to the degree that arrays begin to outcompete the X for DCC binding, as demonstrated by the weaker X chromosome staining relative to array staining. **e**, When both A motifs in *rex-1*•60 are mutated, DCC recruitment to the arrays is severely reduced, and X chromosome staining is restored. **f**, **g**, *rex-1*•241 (**f**) and *rex-1*•148 (**g**) each contain four A motifs as well as two or one B motifs, respectively; both exhibit maximum recruitment strength, completely outcompeting the X for DCC staining. **h**, Loss of the only B motif in *rex-1*•148 (*rex-1*•148 mB_2) reduces recruitment but does not eliminate it. **i**, Map of *rex-1* fragments used in this paper. Red circles represent A motifs; blue squares represent B motifs. Stronger recruitment is indicated by darker green. Scale bar, 2 μm.

Figs 2c, g, h). Mutation of the single B in *rex-1*•33 (*rex-1*•33mB$_2$, with 1A,0B motifs) nearly eliminated DCC binding (category 1, 9% recruitment). However, the addition of three A motifs, as in *rex-1*•148mB$_2$ (4A,0B motifs), partly restored binding (category 2, 100% recruitment). The B$_2$ mutation could not be suppressed further by extending *rex-1* to include an additional B motif (*rex-1*•241mB$_2$, with 4A,1B motifs), indicating at least some dependence of DCC recruitment on relative motif positions as well as absolute motif number.

Our cumulative results show that at least two disparate DNA motifs, probably recognized by different proteins (or possibly RNAs) act in combination to recruit the DCC. The involvement of co-occurring motifs increases the specificity and potentially the stability of DCC binding. Furthermore, each motif class provides a separate opportunity to enlist regulatory factors in X repression. Despite the participation of two motifs in recruitment, multiple A motifs can recruit the DCC in part even without motif B. Cooperativity in DCC binding to neighbouring A motifs could account for the potency of multiple A motifs in DCC recruitment and their partial ability to overcome the loss of motif B. Alternatively, if a motif-B-binding factor is essential for DCC recruitment, it might be brought to *rex* sites through association with motif-A-binding factors and this interaction stabilized through motif B binding.

Our work has decoded essential *cis*-acting information that directs the *C. elegans* dosage compensation complex to repress X-chromosome gene expression. Remarkably, X-specific repression is established through sequences not specific to the X chromosome. *rex* sites enriched for the co-occurrence of at least two prevalent motifs mark X chromosomes as targets for DCC binding. Additional features, possibly including chromatin modifications or other regulatory sequences, might synergize with *rex* sites to permit DCC binding on X and prevent it on autosomes. Widely dispersed *rex* sites, in the context of X, recruit the DCC and probably nucleate DCC spreading to neighbouring areas that cannot independently bind the DCC. In this manner, the arrangement of common motifs induces chromosome-wide repression.

Recent studies of dosage compensation in *Drosophila melanogaster* identified X fragments bound by the MSL (male-specific lethal) complex[17–20], a male-specific RNA–protein complex that increases transcription from the single male X chromosome. Computational analysis[17,18] of these fragments, bound through initial MSL recruitment or subsequent MSL spreading, identified many combinations of shared, degenerate motifs, but none were specific to X. If mutational analysis proves the fly motifs to be essential for MSL binding, as we have shown for worm motifs in DCC recruitment, remarkably similar principles would seem to govern the X-specific binding of two evolutionarily unrelated protein complexes that regulate whole chromosomes in opposite ways.

METHODS

Motifs. Motif finding was performed with MEME[15] on the four *rex* sequences. Starting parameters were selected to maximize the recovery of motifs that conform to a priori expectations for binding sites of sequence-specific DNA-binding proteins, including degenerate DNA motifs 6–16 bp in length, occurring on either strand, often repeated multiple times in a local region of DNA. From models trained under these initial conditions, the two most consistently high-scoring candidate motifs, A and B, were chosen for functional analysis (Supplementary Methods). Patser[21] was used to scan all sequence data sets against position weight matrices for motifs A and B.

Recruitment sites. *rex* sequences reside at the following X chromosome coordinates: *rex-1*•241, X:4395434,4395674; *rex-2*•147, X:1908940,1909087; *rex-3*•115, X:11361205,11361319; and *rex-4*•411, X:11521745,11522155. They can be downloaded from http://www.wormbase.org. Nucleotide sequences of smaller *rex-1* fragments are given in Supplementary Methods.

Received 10 July; accepted 11 October 2006.
Published online 19 November 2006.

1. Grewal, S. I. S. & Elgin, S. C. R. Heterochromatin: new possibilities for the inheritance of structure. *Curr. Opin. Genet. Dev.* **12,** 178–187 (2002).
2. Yamada, T., Fischle, W., Sugiyama, T., Allis, C. D. & Grewal, S. I. S. The nucleation of heterochromatin by a histone deacetylase in fission yeast. *Mol. Cell* **20,** 173–185 (2005).
3. Reik, W. *et al.* Chromosome loops, insulators, and histone methylation: new insights into regulation of imprinting in clusters. *Cold Spring Harb. Symp. Quant. Biol.* **69,** 29–37 (2004).
4. Nusinow, D. A. & Panning, B. Recognition and modification of sex chromosomes. *Curr. Opin. Genet. Dev.* **15,** 91–122 (2005).
5. Lucchesi, J. C., Kelly, W. G. & Panning, B. Chromatin remodeling in dosage compensation. *Annu. Rev. Genet.* **39,** 615–651 (2005).
6. Meyer, B. J. X-chromosome dosage compensation. ⟨http://www.wormbook.org/chapters/www_dosagecomp/dosagecomp.html⟩ (2005).
7. Chuang, P.-T., Albertson, D. G. & Meyer, B. J. DPY-27: a chromosome condensation protein homolog that regulates *C. elegans* dosage compensation through association with the X chromosome. *Cell* **79,** 459–474 (1994).
8. Lieb, J. D., Albrecht, M. R., Chuang, P.-T. & Meyer, B. J. MIX-1: An essential component of the *C. elegans* mitotic machinery executes X chromosome dosage compensation. *Cell* **92,** 265–277 (1998).
9. Losada, A. & Hirano, T. Dynamic molecular linkers of the genome: the first decade of the SMC proteins. *Genes Dev.* **19,** 1269–1287 (2005).
10. Bhalla, N., Biggins, S. & Murray, A. W. Mutation of YCS4, a budding yeast condensin subunit, affects mitotic and nonmitotic chromosome behavior. *Mol. Biol. Cell* **13,** 632–645 (2002).
11. Dej, K. J., Ahn, C. & Orr-Weaver, T. L. Mutations in the *Drosophila* condensin subunit dCAP-G: defining the role of condensin for chromosome condensation in mitosis and gene expression in interphase. *Genetics* **168,** 895–906 (2004).
12. Cobbe, N., Savvidou, E. & Heck, M. M. Diverse mitotic and interphase functions of condensins in *Drosophila. Genetics* **172,** 991–1008 (2006).
13. Csankovszki, G., McDonel, P. & Meyer, B. J. Recruitment and spreading of the *C. elegans* dosage compensation complex along X chromosomes. *Science* **303,** 1182–1185 (2004).
14. Dawes, H. E. *et al.* Dosage compensation proteins targeted to X chromosomes by a determinant of hermaphrodite fate. *Science* **284,** 1800–1804 (1999).
15. Bailey, T. L. & Elkan, C. in *Proceedings of the Second International Conference on Intelligent Systems for Molecular Biology* (eds Altman, R., Brutlag, D., Karp, P., Lathrop, R. & Searls, D.) 28–36 (AAAI Press, Menlo Park, California, 1994).
16. Miller, L. M., Plenefisch, J. D., Casson, L. P. & Meyer, B. J. *xol-1*: a gene that controls the male modes of both sex determination and X chromosome dosage compensation in *C. elegans. Cell* **55,** 167–183 (1988).
17. Dahlsveen, I. K., Gilfillan, G. D., Shelest, V. I., Lamm, R. & Becker, P. B. Targeting determinants of dosage compensation in *Drosophila. PLoS Genet.* **2,** e5 (2006).
18. Gilfillan, G. D. *et al.* Chromosome-wide gene-specific targeting of the *Drosophila* dosage compensation complex. *Genes Dev.* **20,** 858–870 (2006).
19. Alekseyenko, A. A., Larschan, E., Lai, W. R., Park, P. J. & Kuroda, M. I. High-resolution ChIP-chip analysis reveals that the *Drosophila* MSL complex selectively identifies active genes on the male X chromosome. *Genes Dev.* **20,** 848–857 (2006).
20. Legube, G., McWeeney, S. K., Lercher, M. J. & Akhtar, A. X-chromosome-wide profiling of MSL-1 distribution and dosage compensation in *Drosophila. Genes Dev.* **20,** 871–883 (2006).
21. Hertz, G. Z. & Stormo, G. D. Identifying DNA and protein patterns with statistically significant alignments of multiple sequences. *Bioinformatics* **15,** 563–577 (1999).

Supplementary Information is linked to the online version of the paper at www.nature.com/nature.

Acknowledgements We thank A. Coulson for cosmids; S. Uzawa for technical innovation with image analysis; P. Nix for help with *xol-1* XO rescue experiments; M. Ralston for statistical analysis; and R. Auty, M. Botchan, S. Brenner, T. Cline, R. Losick, E. Ralston and A. Severson for comments on the manuscript. This work was supported by an NIH grant (B.J.M.), NIH training grants (P.M. and B.K.P.), and a Netherlands Organisation for Scientific Research (NWO) Talent fellowship (J.J.). B.J.M. is an investigator and J.J. an associate of the Howard Hughes Medical Institute.

Author Information Reprints and permissions information is available at www.nature.com/reprints. The authors declare no competing financial interests. Correspondence and requests for materials should be addressed to B.J.M. (bjmeyer@berkeley.edu).